

## Electronic Supplementary Information

### A “Turn-on” Carbon nanotube-Ag Nanoclusters Fluorescent Sensor for Sensitive and Selective Detection of Hg<sup>2+</sup> with Cyclic Amplification of Exonuclease III Activity

Guangfeng Wang\*<sup>‡</sup>, Gang Xu<sup>‡</sup>, Yanhong Zhu, Xiaojun Zhang\*

*Key Laboratory of Chem–Biosensing, Anhui province; Key Laboratory of Functional Molecular Solids, Anhui province; College of Chemistry and Materials Science, Anhui Normal University, Center for nanoscience and nanotechnology, Anhui Normal University, Wuhu 241000, P R China*

#### 1. Experiment sections

##### 1.1. Materials

HPLC-purified thymine-rich single strand DNA oligonucleotides S1 with specific sequence (5'-CCCCCCCCCTTCGTTTCGTTCCCTTCGTTTCGTT-3') were obtained from Sangon Biotechnology Co. Ltd. (Shanghai, China). CNTs (single-walled carbon nanotubes, diameter  $\leq$  5 nm, lengths 5-15  $\mu$ m) were purchased from Sangon Biotechnology Co. Ltd. (Shanghai, China). Exo III, Phosphate-buffered saline (PBS, pH 7.4, 10 mM if not illustrated), and other reagents were obtained from the Sinopharm Chemical Reagent Co. Ltd. (Shanghai, China). All chemicals were of analytical grade or better and were used without further purification. Ultrapure water was used throughout all experiments.

##### 1.2. Apparatus

Fluorescence spectra were recorded on F-4600 FL Spectrophotometer (Hitachi, Japan) equipped with a quartz cell (1cm $\times$ 1cm) in the fluorescence mode an excitation wavelength of 580 nm. Ultraviolet-visible absorption spectra were measured on UV-3010 spectrophotometer (Hitachi, Japan). High-resolution transmission electron microscope (HRTEM) observations for the morphological measurements of AgNCs-T-rich S1 were performed on JEOL-2010F with an acceleration voltage of 200 KV. Decay curves measurements were performed with the time correlated single photo counting technique on the combined steady state and lifetime spectrometer (Edinburgh Analytical Instruments, FLS920). Ultrapure water was obtained through PSDK2-10-C (Beijing, China). All electrochemical measurements were performed using a CHI 660B (Shanghai Chen Hua Instrument Co. Ltd.) electrochemical workstation in a conventional three-electrode system with glassy carbon electrode (GCE) as working electrodes, a saturated calomel electrode (SCE) as reference electrode and the platinum foil electrode as counter electrode. Photos were taken by MEIZU MX2 (Zhuhai, China). All pH measurements were measured with a Model pHs-3c meter (Shanghai, China). All optical measurements were performed with slit information that EX Slit=2.5 nm, EM Slit=5.0 nm at room temperature under ambient conditions.

##### 1.3. Synthesis of oligonucleotide-stabilized Ag nanoclusters (AgNCs-T-rich S1)

The oligonucleotide-stabilized Ag nanoclusters were synthesized according to previous reports.<sup>1</sup>

Briefly, AgNO<sub>3</sub> in a molar ratio of 6 : 1 was added to a 10 mM T-rich S1 solution (dissolved in PBS) followed by the vigorous shaking of the solution for 30 sec. After stirring, freshly prepared NaBH<sub>4</sub> (10 μL) with the same concentration (60 mM) was added into this mixture for reduction followed by vigorous shaking of the mixture for 30 sec and the reduced oligonucleotide-Ag solution was incubated at 4 °C and allowed to react for 1 h in the dark. Silver ions bound with cytosine<sup>2</sup> were reduced to form nanoclusters. AgNCs-T-rich S1 was synthesized and would be utilized for further fluorescence detection.

#### 1.4. Electrochemical characterization of AgNCs-T-rich S1

To verify whether AgNCs-T-rich S1 was synthesized successfully as we designed, electrochemical characterization was processed. 20 μL AgNCs-T-rich S1 (10 μM) were dropped onto the cleaned GCE and dried for about 6 h at room temperature naturally for the cyclic voltammetry (CV) study. Then electrochemical CV measurement from -500 mV to 600 mV (vs. SCE) (scan rate: 50 mV/s) was carried out in PBS.

#### 1.5. Analysis of Hg<sup>2+</sup> with AgNCs-T-rich S1/CNTs

The purified CNTs were sonicated in DMF for 1 h to give a homogeneous black solution and stored for use. 20 μL CNTs (10 μM) solution was added to 80 μL PBS buffer containing 10 μM AgNCs-T-rich S1 and then the mixture was allowed to incubate for 30 min at room temperature in dark environment. The resulting AgNCs-T-rich S1/CNTs hybrids solution was used directly for Hg<sup>2+</sup> detection assay. Then various concentrations of Hg<sup>2+</sup> ions were added to 100 μL reaction buffer (PBS) containing 100 Units Exo III and 10 μM AgNCs-T-rich S1/CNTs and the resultant mixture was incubated at 37 °C for 2 h followed by heated to 80 °C for 10 min to inactivate the Exo III. All the sample solutions were allowed to slowly equilibrate to room temperature for about 20 min and then the fluorescence intensity is measured and plotted. For the study of the role of Exo III, in control experiment, the detection process was all the same with the above except the addition of Exo III.

#### 1.6. Real sample analysis

Fifteen river water samples were collected respectively at five sewage outfalls along the Qingyi River, Yangzi River (Wuhu) and Yushan Lake (Maanshan), and then were filtered through a 0.2 μm membrane to remove oils and other organic impurities. For the recovery test, the spiked water samples were diluted with equal volume of PBS. Subsequently, the river water samples were spiked with standard solutions of Hg<sup>2+</sup> over the concentrations from 0.1 to 100 nM prior to fluorescence measurement.

## 2. Results and discussion

### 2.1. Characterization of the AgNCs-T-rich S1

#### 2.1.1. Electrochemical characterization

Electrochemical experiments were performed to verify the electrochemical propriety of the synthesized AgNCs in T-rich S1. As Fig. 1A shows, the CV obtained has an oxidation peak at about 0.37 V and a reduction peak at 0 V nearby. It shows the existence of the anodic process corresponding to the metal-based oxidation of the nanoclusters ( $n \text{ Ag} \rightarrow n \text{ Ag}^+ + e^-$ ). When the

$\text{Ag}^+$  species is rapidly consumed in an electrochemically coupled reaction up on the anodic cycle, some cathodic activity for a subsequent reduction ( $n \text{Ag}^+ + e^- \rightarrow n \text{Ag}$ ) can be seen as well. Once we substitute AgNCs-T-rich S1/GCE by AgNCs-T-rich S1/CNTs/GCE, we can see both oxidation peak and reduction peak is gone which may be ascribed to the effect of CNTs. The adsorbed AgNCs-T-rich S1 on the CNTs surface make electron transfer from AgNCs to CNTs directly resulting that there is no characteristic peak corresponding to AgNCs on CV. So we can conclude that AgNCs was labeled onto T-rich S1 successfully and there is an ET process when CNTs was added.

### 2.1.2. Optical characterization

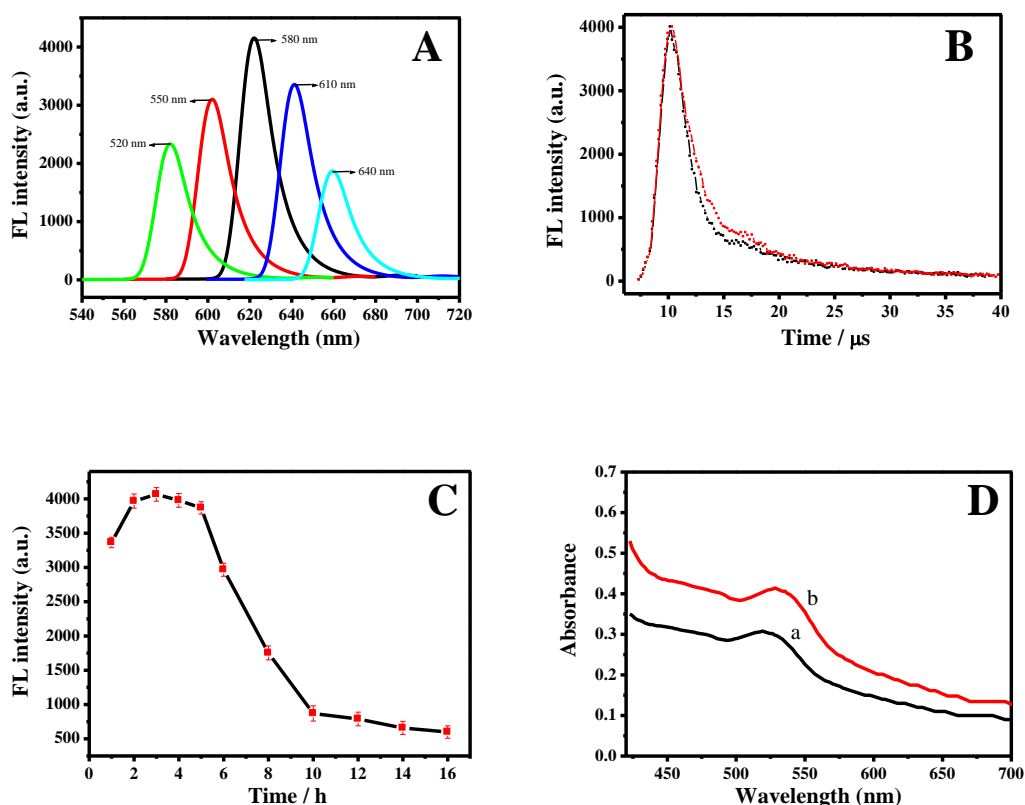


**Fig. S1** (A) Fluorescence emission spectra of obtained AgNCs-T-rich S1 under different excitation wavelengths. (B) Fluorescence decay of AgNCs-T-rich S1 in the (black) absence and (red) presence of  $\text{Hg}^{2+}$ . (C) Time evolution of the fluorescence intensity of AgNCs-T-rich S1. Fluorescence intensity was recorded at 626 nm with an excitation wavelength of 580 nm. (D) UV-visible absorbance spectra of AgNCs-T-rich S1 (a) and AgNCs-T-rich S1/CNTs (b).

### 2.1.3. HRTEM characterization

As characterized by HRTEM (Fig. S2), in general, the AgNCs was shown to be individual spherical and uniform. In some cases, a small number of Ag nanoparticles for larger or aggregated clusters are detected as well.

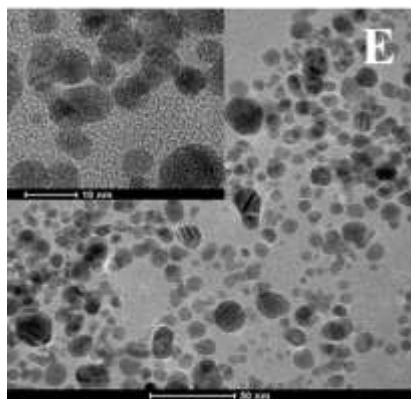


**Fig. S2** HRTEM images of the synthetic AgNCs-T-rich S1.

### 2.2. The kinetic behaviors of AgNCs-T-rich S1/CNTs

The kinetic behaviors of AgNCs-T-rich S1/CNTs with various concentrations of  $\text{Hg}^{2+}$  in the presence of 100 U Exo III are studied. Fig. 3A shows fluorescence reappearing of AgNCs-T-rich S1/CNTs as a function of incubation time. In the reaction solution containing 80 nM  $\text{Hg}^{2+}$ , the fluorescent intensity exhibits a rapid rising in the first 50 min and a slow increasing over the last 10 min period. It is hypothesized that the surface effect between carbon nanotubes and AgNCs-T-rich S1 with a large conjugate plane has been broken.<sup>3</sup> The self-folded AgNCs-T- $\text{Hg}^{2+}$ -T S1 released from CNTs automatically should be the main reason for the higher fluorescence. With the digestion of duplex-like AgNCs-T- $\text{Hg}^{2+}$ -T S1, the cycle of  $\text{Hg}^{2+}$  is formed and then plays an amplified role. In the presence of various concentrations of  $\text{Hg}^{2+}$ , fluorescence intensity increase of AgNCs-T-rich S1/CNTs is consistent with that of 80 nM as Inset of Fig. 3A shows. Thus, we can conclude that the formation of duplex-like AgNCs-T- $\text{Hg}^{2+}$ -T S1 reduces the absorbance of AgNCs-T-rich S1 onto the CNTs and reduces fluorescence quenching efficiency. Thus an overall fluorescence increase which displays fluorescence enhancement compared to that without  $\text{Hg}^{2+}$  is contributed. The experimental results demonstrate that the “turn-on” fluorescence of AgNCs-T-rich S1/CNTs approach could be used as a sensitive approach for  $\text{Hg}^{2+}$  detection in aqueous solution.

### 2.3. Optimization of assay conditions

The fluorescence emission properties of AgNCs-T-rich S1/CNTs with  $\text{Hg}^{2+}$  in the presence of Exo III are sensitive to the pH value of the reaction solution. For the optimization study, Fig. S3 depicts the relationship between different pH value of reaction solution from 4 to 12 and the fluorescence intensity. As Fig. S3A shows, fluorescence intensity increases with pH and reached a plateau when the pH is about 7.0. The fluorescence intensity decreased gradually while at relatively higher pH (>8.0). Combined the previous reports<sup>4</sup> with our data of pH optimization, an ideal pH value of 7.4 is chosen for the next assay experiments. Also, because of the existence of Exo III, an enzyme which has a high exodeoxyribonuclease activity, the temperature of the reaction solution is investigated to find an ideal temperature from 25 °C to 50 °C. As Fig. S3B shows, 37 °C at which the fluorescence intensity is the highest is chosen as the reaction

temperature in the assays.

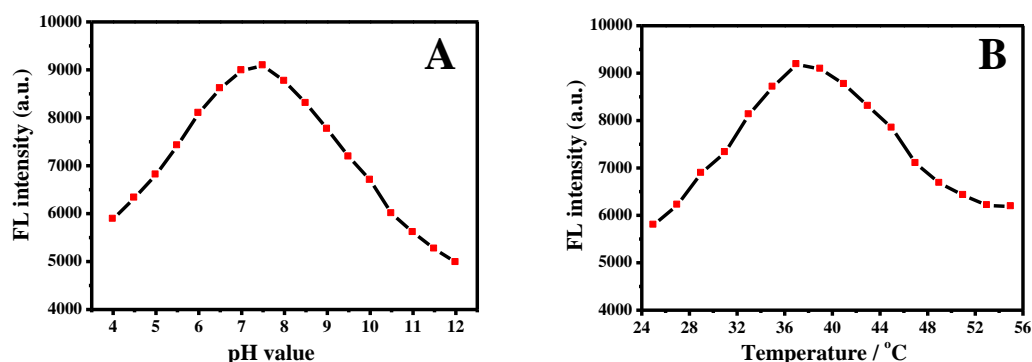


**Fig. S3** (A) Fluorescence intensity of AgNCs-T-rich S1/CNTs as a function of pH value of the reaction solution containing 250 nM  $\text{Hg}^{2+}$  ions, 100 U Exo III for 60 min at 37 °C. (B) Fluorescence intensity of AgNCs-T-rich S1/CNTs as a function of temperature of the reaction solution (pH 7.4) containing 200 nM  $\text{Hg}^{2+}$  ions, 100 U Exo III for 60 min. Fluorescence intensity was recorded at 626 nm with an excitation wavelength of 580 nm.

#### 2.4. Selectivity of the “turn-on” fluorescent sensor

The selectivity of the detection sensor was tested by substituting the  $\text{Hg}^{2+}$  in the system with various metal ions which were commonly present in real samples, such as  $\text{Ag}^+$ ,  $\text{Pb}^{2+}$ ,  $\text{Mn}^{2+}$ ,  $\text{Zn}^{2+}$ ,  $\text{Ni}^{2+}$ ,  $\text{Cu}^{2+}$ ,  $\text{Fe}^{2+}$ ,  $\text{Fe}^{3+}$  and  $\text{Cd}^{2+}$ . Each reaction mixtures containing 10  $\mu\text{M}$  AgNCs-T-rich S1/CNTs, 100 Units Exo III,  $\text{Hg}^{2+}$  ions (20, 40 and 60 nM) or each competing metal ion (5, 10 and 15  $\mu\text{M}$ ) was incubated at 37 °C for 60 min. As shown in Fig. S4, it can be seen that all the other metal ions present only slight and negligible effects on the fluorescence of the AgNCs-T-rich S1/CNTs detection system and none of the tested metal ions give fluorescence intensity higher than half of that produced by 20 nM  $\text{Hg}^{2+}$  ions. Such excellent selectivity is attributed to the specific T- $\text{Hg}^{2+}$ -T base pairing and this approach has great potential for further use.

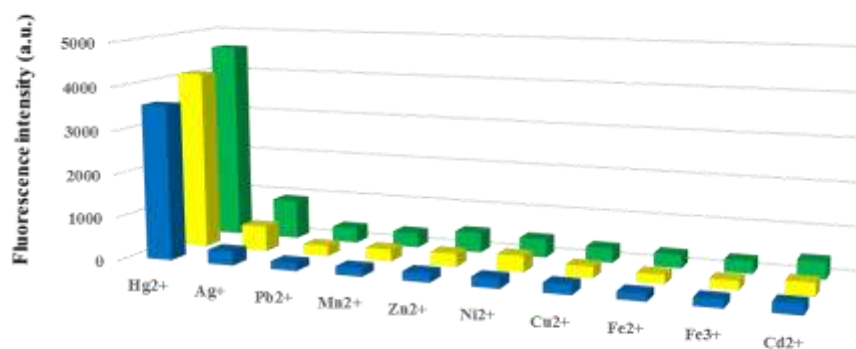


**Fig. S4** The effect of different metal ions (5, 10 and 15  $\mu\text{M}$ ) on the fluorescence emission of AgNCs-T-rich S1/CNTs compared with  $\text{Hg}^{2+}$  ions (20, 40 and 60 nM). Fluorescence intensity was recorded at 626 nm with an excitation wavelength of 580 nm.

## 2.5. Real sample analysis

To study the actual application of this  $\text{Hg}^{2+}$  sensor, we investigated the kinetic studies in real samples of Qingyi River. We added 50 nM  $\text{Hg}^{2+}$  into river samples and measured the fluorescence intensity every 10 min. The result is shown below.

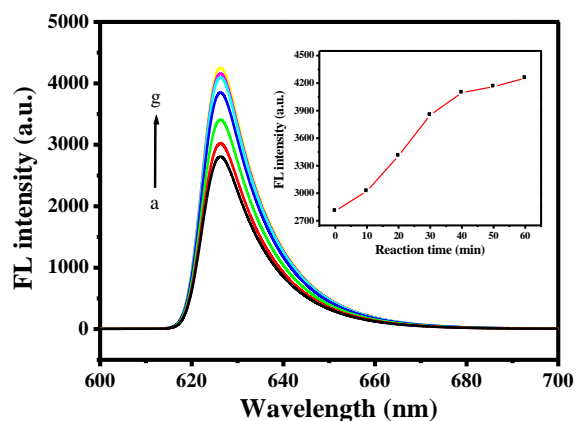


**Fig. S5** Our kinetic studies of the reappearing effect of  $\text{Hg}^{2+}$  on AgNCs-T-rich S1/CNTs. (a-g): Fluorescence emission spectra of AgNCs-T-rich S1/CNTs in the presence of 50 nM  $\text{Hg}^{2+}$  with scan times from 0 to 60 min (scan interval: 10 min). Inset: Fluorescence intensity of AgNCs-T-rich S1/CNTs as a function of time with 50 nM  $\text{Hg}^{2+}$  in the real samples.

What's more, as an excellent sensor, it should not be disturbed by other coexisting ions. In this case, an interference study of coexisting ions with the  $\text{Hg}^{2+}$  at the same time in real samples (Qingyi River) was performed to further investigate the specificity of our sensor in the presence of other coexisting ions. The detailed information was shown as Fig. S6.

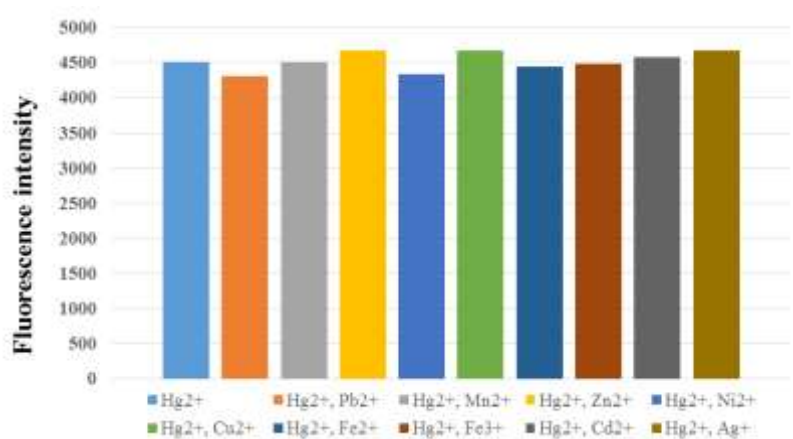


**Fig. S6** Interference study in the real samples analysis of  $\text{Hg}^{2+}$  by this fluorescent biosensor.

Number of Qingyi River	Added (nM)	Founded(nM) (mean <sup>a</sup> ± SD <sup>b</sup> )	Recovery
1	0.5	0.467±0.07	0.934
2	2	1.93±0.12	0.965
3	10	9.5±1.3	0.950
4	50	51.8±3.12	1.036
5	100	98.5±8	0.985

Number of Yangzi River	Added (nM)	Founded(nM) (mean <sup>a</sup> ± SD <sup>b</sup> )	Recovery
1	0.5	0.488±0.12	0.976
2	2	1.96±0.19	0.980
3	10	10.2±1.1	1.020
4	50	51.3±3.2	1.026
5	100	102±7.5	1.020

Number of Yushan Lake	Added (nM)	Founded(nM) (mean <sup>a</sup> ± SD <sup>b</sup> )	Recovery
1	0.5	0.477±0.09	0.954
2	2	2.07±0.11	1.035
3	10	9.67±2.1	0.967
4	50	51.1±2.3	1.022
5	100	103±6.4	1.030

a Mean of 5 determinations.

b SD, standard deviation.

**Table S1** Determination results of Hg<sup>2+</sup> added in Qingyi River, Yangzi River and Yushan Lake.

### 3. Reference

1. (a) C. I. Richards, S. Choi, J. C. Hsiang, Y. Antoku, T. Vosch, A. Bongiorno, Y. L. Tzeng and R.M. Dickson, *J. Am. Chem. Soc.*, 2008, **130**, 5038. (b) B. Sengupta, C. M. Ritchie, J. G. Buckman, K. R. Johnsen, P. M. Goodwin and J. T. Petty, *J. Phys. Chem. C*, 2008, **112**, 18776.
2. A. Ono, S. Cao, H. Togashi, M. Tashiro, T. Fujimoto, T. Machinami, S. Oda, Y. Miyake, I. Okamoto and Y. Tanaka, *Chem. Commun.*, 2008, **21**, 4825.
3. (a) L. B. Zhang, T. Li, B. L. Li, J. Li and E. K. Wang, *Chem. Commun.*, 2010, **46**, 1476. (b) Y. Miyake, H. Togashi, M. Tashiro, H. Yamaguchi, S. Oda, M. Kudo, T. Fujimoto, T. Machinami and A. Ono, *J. Am. Chem. Soc.*, 2006, **128**, 2172. (c) X. Gao, G. Xing, Y. Yang, X. Shi, R. Liu, W. Chu, L. Jing, F. Zhao, C. Ye, H. Yuan, X. Fang, C. Wang and Y. Zhao, *J. Am. Chem. Soc.*, 2008, **130**, 9190.
4. (a) G.F. Wang, G. Xu, X. Zhou, G. Zhang, H. Huang, X.J. Zhang and L. Wang, *Talanta*, 2013, **103**, 75. (b) H.Z. Sun, H.T. Wei, H. Zhang, Y. Ning, Y. Tang, F. Zhai and B. Yang, *Langmuir*, 2011, **27**, 1136.